Journal of Alloys and Compounds 509 (2011) 1305–1309

Contents lists available at ScienceDirect

Journal of Alloys and Compounds

journal homepage: www.elsevier.com/locate/jallcom

Semiconductor-septum solar rechargeable storage cells

R.R. Sawant, S.S. Shinde, C.H. Bhosale, K.Y. Rajpure*

Electrochemical Materials Laboratory, Department of Physics, Shivaji University, Kolhapur 416 004, India

ARTICLE INFO

Article history:
Received 5 May 2010
Received in revised form 5 October 2010
Accepted 6 October 2010
Available online 14 October 2010

Keywords:
$CdIn_2S_4$ thin films
SEM
EDAX
SC-SEP storage cell
Photoelectrochemical technology

ABSTRACT

We have investigated the production of energy as well as its storage using semiconductor-septum solar cells using $CdIn_2S_4$ thin films. The thin films of $CdIn_2S_4$ as a septum have been deposited by using spray pyrolysis technique on to the stainless steel substrates. The semiconductor-septum solar rechargeable (SC-SEP) storage cell is engineered with the configuration C|1 M polysulphide|n-$CdIn_2S_4$|stainless steel||1 M $FeCl_3$ or 1 M $K_4Fe(CN)_6$|C. The study of charging and discharging modes are exhaustively argued. The $FeCl_3$ based storage cell has superior efficiency for solar conversion energy than other electrolytes. The deposited $CdIn_2S_4$ was successfully used as a working electrode in semiconductor-septum storage cell.

1. Introduction

The recent awakening to the urgency for cleansing the polluted environment and the avoidance of further pollution (i.e., global warming), as evident during the environmental climate change conference (December, 6–18, 2009 at Copenhagen), has rekindled interest in clean, nonpolluting and renewable energy sources for generating the two most commercial forms of energy, i.e., electricity and fuel. Because of the depleting, dirty (pollution) and dangerous characteristics of fossil and nuclear fuels, which presently form the base for the commercial energies, there is an ongoing search for clean and renewable energies. In this respect, solar energy is unique in that it is inexhaustible, nonpolluting and does not contribute to global warming. Solar energy conversion devices can replace the present day energy generating process of burning fossil fuels or smashing atoms. These solar energy conversion devices can be classified into two major groups: (a) solar thermal conversion devices using the infrared part (49%) of the solar spectrum, e.g., solar heat collector, and (b) solar photon conversion devices utilizing visible/near-ultraviolet region (51%) of solar spectrum. The solar photon conversion devices called solar cells can be classified into three main categories, (i) Solid-state photovoltaic (p/n junction) solar cells, (ii) metal-semiconductor based Schottky barrier (M-S) solar cells, and (iii) semiconductor liquid junction based photoelectrochemical (PEC) solar cells [1–3]. The semiconductor liquid junction photoelectrochemical solar cells fall in between solid-state photovoltaics and nature's photosynthetic systems. The solid-state photovoltaic solar cells are well suited for special applications, e.g., for supplying power to space vehicles and to remote inaccessible localities. In contrast to solid-state photovoltaic devices, semiconductor liquid junction based photoelectrochemical solar cells are relatively inexpensive involving convenient and economically viable material synthesis and tailoring processes and are easy to fabricate because they require mere immersion of the desired photoactive semiconductor into the electrolyte solution containing a suitable redox couple. The most important and vital advantage in photoelectrochemical solar cells is the possibility of in situ storage. Energy storage plays important roles in conserving available energy and improving its utilization, since many energy sources are intermittent in nature. Short-term storage of only a few hours is essential in most applications; however, long-term storage of a few months may be required in some applications.

The semiconductor–liquid junction photoelectrochemical solar cell consists of photoactive semiconductor (SC) electrode immersed in electrolytic solution containing a suitable redox couple and counter electrode which can be a metal or semiconductor. The irradiation of semiconductor electrolyte junction with light of $h\nu > E_g$ (E_g is the band gap of SC) results in generation and separation of charge carriers. The minority carriers, e.g., hole (h^+) in n-type SC, migrate to electrolyte and take part in the electrochemical reaction. The majority carriers, e.g., electrons (in n-type SC), go to the counter electrode through an external circuit and take part in the counter reaction. Accordingly, in recent years, the study of rechargeable storage cells has attracted much attention [4–6]. During the past decades, many efforts, such as developing new intercalated cathode, searching carbon alternatives and enhance the stability of electrolyte, have been made to improve the per-

---

* Corresponding author. Tel.: +91 231 2609435; fax: +91 231 2691533.
E-mail address: rajpure@yahoo.com (K.Y. Rajpure).

0925-8388/$ – see front matter © 2010 Elsevier B.V. All rights reserved.
doi:10.1016/j.jallcom.2010.10.020

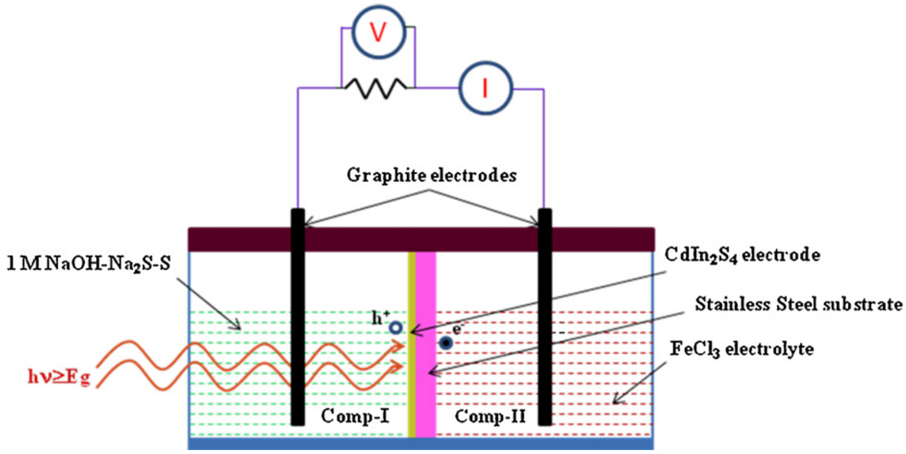

Fig. 1. Schematic diagram of semiconductor-septum solar rechargeable storage cell.

formance of rechargeable storage cells. However, an alternative strategy has been suggested in which a PEC cell has been used which offers possibility of both solar energy conversion and storage. PEC cells have been used in rechargeable electrochemical storage, septum cells and redox couple storage devices. In the rechargeable electrochemical storage cells, the storage electrode capable of undergoing reversible chemical change is used [7,8]. The solar energy storage with the help of semiconductor-septum (SC-SEP) cells is most attracting and promising due to its inherent properties. The concept of using semiconductor-septum in an energy storage device is based on modeling of natural photosynthetic system with pigmented bilayer lipid membrane [9]. Tien and Chen [10] have reported on the septum cell for photoelectrolysis of seawater. This cell consists of CdSe deposited over Ni foil and a Pb as counter electrode. The CdSe side contains ferro/ferri cyanide and Ni side contains seawater as an electrode. Jackowaska and Tien [11] have developed a septum cell in which the PEC cell consists of two chambers with the configuration CdS|polysulphide|Pt||CuNO$_3$|Cu. CdSe (pellets). semiconductor-septum PEC cells with configuration M$_1$|1 M Na$_2$S, 1 M NaOH||CdSe||0.5 M AgNO$_3$|M$_2$, where M$_1$ = SCE, Cu$_2$S and Pt and M$_2$ = Pt, Pb and Ag, have been constructed by Xiao and Tien [12] and their PEC characteristics studied using cyclic voltammetry. Murali et al. [7] have reported on an electrodeposited CdSe septum of 25 cm^2 area. Rajpure and Bhosale [13] have reported Sb$_2$S$_3$ based solar rechargeable SC-SEP cell. Variety of semiconductors viz. CdS, CdSe, Cd$_2$SnO$_4$, Sb$_2$S$_3$, Sb$_2$Se$_3$, CdTe, Fe$_2$O$_3$, CdIn$_2$S$_4$, etc. are used as a semiconductor-septum with different electrolyte combinations. These materials are prepared by using various techniques such as electrodeposition [14], chemical bath deposition [15], spray pyrolysis [16], mechanical pressing [11,12], etc.

In the present manuscript we report on the spray deposited n-CdIn$_2$S$_4$ thin films on to the stainless steel substrates and their use as septum electrode in redox storage cells for the first time. These films are used as a separator in the rechargeable storage cell. The renewed efforts are directed towards the combinations of n-CdIn$_2$S$_4$ and various electrolytes are discovered that could affect the stable conversion of light into electricity or fuels as well as storage at these systems. The charging of SC-SEP redox storage cells upon illumination and their subsequent electrochemical discharge are studied and argued in detail.

2. Experimental

The CdIn$_2$S$_4$ electrodes were deposited on to preheated stainless steel (SS) substrates by taking equimolar aqueous solutions of analytical grade Cadmium Chloride (CdCl$_2$), Indium trichloride (InCl$_3$) and Thiourea [CS(NH$_2$)$_2$] in appropriate volumes to obtain Cd:In:S ratio as 1:2:4, respectively, at optimized substrate temperature (270 °C for SS substrate) and solution concentration (0.05 M). The spray rate of this solution was kept constant ~3 cc min^{-1}, nozzle to substrate distance was 32 cm and spray nozzle moved back and forth over the substrate with frequency 0.29 Hz. These prepared films are used as a semiconductor electrode in septum solar cells.

When a semiconductor electrode is taken as a separator of two compartments containing aqueous electrolytes in PEC cells, it is called semiconductor-septum solar cell. The structure of developed n-CdIn$_2$S$_4$ rechargeable storage cell is shown in Fig. 1, can be summarized as: (I) an aqueous electrolyte 1 M polysulphide (NaOH–Na$_2$S–S) in photoelectrode compartment (II) various aqueous electrolytes 1 M FeCl$_3$, K$_4$Fe(CN)$_6$, FeCl$_2$, etc. in the redox compartment. (II) The n-CdIn$_2$S$_4$ semiconductor as a separator of two compartments, i.e., semiconductor-septum. (III) Inert metallic electrodes as an anode, respectively. The cadmium indium sulphide thin films were deposited by a simple and inexpensive spray pyrolysis technique by keeping the preparative parameters at optimized conditions as published elsewhere [17–19], except thin film deposition area. For the construction of semiconductor-septum rechargeable storage cell, we have coated 4 cm × 2.5 cm area of CdIn$_2$S$_4$ thin film on to the stainless steel substrate. Then this septum was inserted in a rectangular box, made up of acrylic (7.5 cm × 2.5 cm × 4.5 cm) to form two compartments. This rectangular box has a 1 cm^2 diameter holes for incorporation of inert metallic electrodes in each compartment of cell. All edges of the rectangular cell and thin film electrode were fixed with epoxy resin (Araldite made in India). A quartz glass window was made to illuminate the CdIn$_2$S$_4$ photoelectrode from one side of compartment. The tungsten lamp (500 W) was used to illuminate the septum electrode. The photoelectrode compartment adjacent to the lamp was filled with 1 M polysulphide (Na$_2$S–NaOH–S) solution and redox compartment was filled with various electrolytes such as FeCl$_3$, K$_4$Fe(CN)$_6$, FeCl$_2$. A water filter was interposed between the cell and light source to avoid heating of the electrolyte. The rechargeablity of the storage cell was studied for charging and discharging modes across load resistance 10 kΩ.

3. Results and discussion

3.1. Morphological study

Scanning electron microscopy is a convenient and versatile tool to study the surface morphology of the film. The surface morphology of the spray deposited CdIn$_2$S$_4$ thin films on to the stainless steel substrates is investigated by scanning electron microscopy. Fig. 2 shows typical SEM image of CdIn$_2$S$_4$ thin film grown on SS substrate prepared at substrate temperature of 270 °C. The micrograph shows surface covered by non-uniformly distributed grains of varying sizes about 150–180 nm. Films are compact and homogenous to the substrate surface. The grain growth is along certain favorable nucleation centers due to which small and large grains are observed. The textured morphology is a consequence of the nucleation of grains that grow geometrically and impinge laterally. The grains observed by SEM are formed by the preferential aggregation of crystallites.

3.2. Compositional analysis

The compositional analysis of the film is carried out by using the EDAX technique for CdIn$_2$S$_4$ film deposited at optimized prepara-

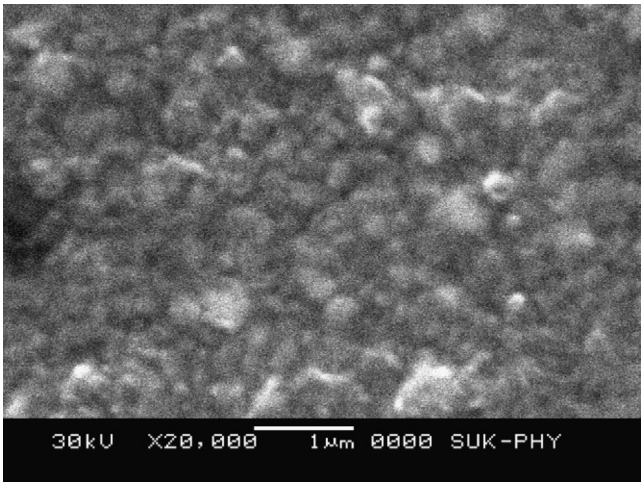

Fig. 2. Typical SEM images of n-$CdIn_2S_4$ thin film deposited on SS substrate.

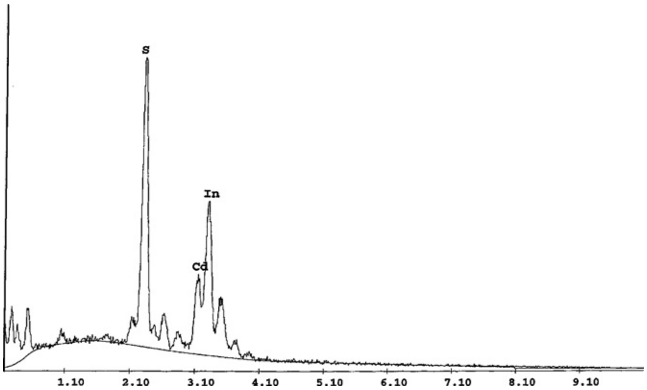

Fig. 3. Energy dispersive analysis by X-rays for $CdIn_2S_4$ thin film deposited on to SS substrates at optimized spray parameters.

tive parameters. Fig. 3 shows a typical EDAX pattern and details of relative analysis of deposited $CdIn_2S_4$ film. The resulting ratio of atomic % of the Cd:In:S has been found to be 1:1.78:3.02 (approximately $CdIn_2S_3$). Table 1 shows that the films are sulphur deficient. Though the air is used to atomize the spray, considering the possibility of oxidation of sulphur at deposition temperature, (270 °C) any oxides of sulphur or other compounds is not detected.

3.3. I–V characteristics

Fig. 4 shows the current–voltage (I–V) characteristics of the PEC solar cell formed with n-$CdIn_2S_4$ electrodes deposited on to SS in dark and light, respectively. The non-symmetric nature of the I–V curves in forward and reverse bias shows the rectification property of semiconductor electrolyte junction. As we illuminate the junction, the I–V curve shifts in fourth quadrant representing that the cell is a generator of electricity. I–V curve in the third quadrant is not influenced much by applied reverse bias, but a large photocurrent flows in the first quadrant. The ideality of junction can be determined using a simple diode equation,

$$I = I_0[e^{eV/nkT} - 1]$$

where n is the junction ideality factor, I_o the reverse saturation current, V the applied forward bias voltage and I the forward current in dark. Under illumination, V and I are replaced by V_L and I_L, respectively.

Table 1
Elemental analysis of $CdIn_2S_4$ thin film with help of EDAX technique.

Element	at.%	K ratio
S	52.18	0.2654
Cd	17.24	0.2436
In	30.59	0.4431
Total	100.00	

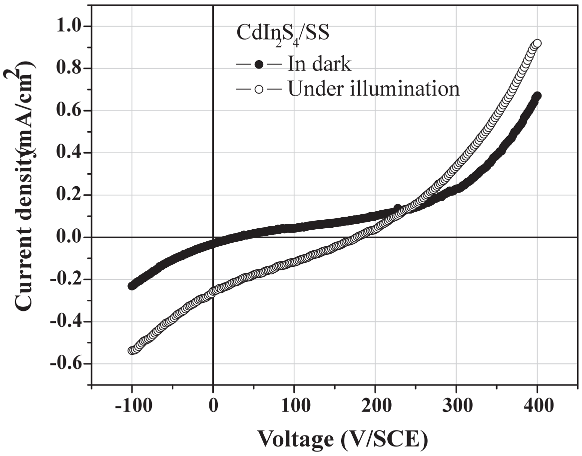

Fig. 4. The current–voltage characteristics of the PEC cell formed with n-$CdIn_2S_4$ electrode deposited on to stainless steel in dark and light.

The junction ideality factors for SS substrates are $n_D = 5.14$ and $n_L = 2.08$. Relatively higher value of junction ideality factors (than 1) indicates the effect of series resistance and carrier recombination mechanism at the semiconductor electrolyte interface [19]. However, the current in reverse bias does not saturate and is attributed to (i) the effective barrier height decrease because of the interfacial layer, (ii) electron–hole pairs are thermally generated in the depletion layer under the condition of large reverse bias and (iii) the current increases due to the onset of the electron injection from an electrolyte because barrier height becomes thin enough for tunneling to take place [20].

3.4. Semiconductor-septum storage cell

The semiconductor-septum storage cell formed with n-$CdIn_2S_4$ electrode is shown in Fig. 1. This type of solar cell is used for the conversion of solar energy into electricity and also able to store the generated electrical energy. When the photosensitive n-type SC electrode is immersed in an electrolyte solution containing a suitable redox system where the Fermi level of the SC is more negative than that of the redox electrolyte (the chemical potential of electrons in the SC and electrolyte is given by the Fermi level and the redox potential, respectively), the equilibration of two chemical potentials occurs by the transfer of electrons from the SC to the electrolyte and it leads to a positive space charge layer in the semiconductor (also called a depletion layer since the region is depleted of majority charge carriers, i.e., electrons in n-type semiconductors). As a result, the conduction and valence band edges are bent upwards in n-type semiconductors, forming a potential barrier against further electron transfer to the electrolyte. Along with the depletion layer in semiconductors, a charged layer known as the Helmholtz layer exists in the electrolyte adjacent to the interface. It consists of charged ions from the electrolyte absorbed on the solid electrode surface. These ions are of opposite sign to the charge induced in the solid electrode. The semiconductor-septum rechargeable storage cell developed with n-$CdIn_2S_4$ electrode causes the generation of electron–hole pairs when the semiconductor electrolyte junction is illuminated with light corresponding to energy $h\nu \geq$ semiconductor band gap. The

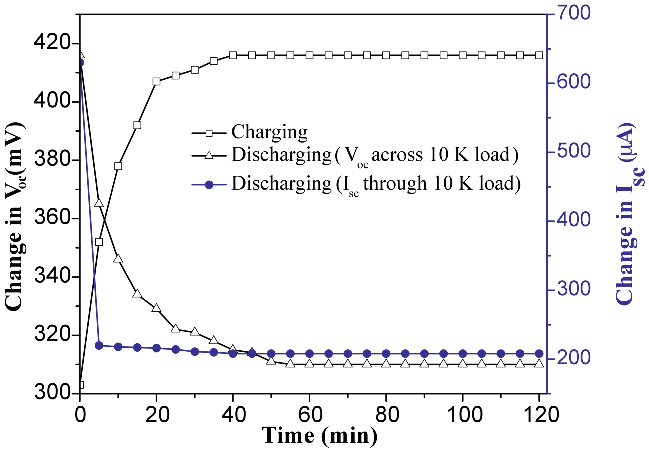

Fig. 5. Variations of voltage and current against time in charging and discharging modes of C|1 M (NaOH–Na_2S–S)|$CdIn_2S_4$||1 M $FeCl_3$|C SC-SEP storage cell.

electron–hole pairs are generated in the semiconductor is separated under the influence of the electric field present in the space charge region. Photons will be absorbed in the depletion layer if their absorption coefficient (α in units of cm^{-1}) is sufficiently large such that $l/\alpha < \omega$ (depletion width). The photovoltage produced in a PEC cell is equal to the difference between the Fermi level in the semiconductor and the redox potential of the electrolyte (as sensed by the metal counter electrode). Photogenerated minority carriers (e.g., holes in n-type SC and electrons in p-type SC) move towards the semiconductor surface where they are consumed for oxidation of reduced species and reduction of oxidized species of the redox system in n-type and p-type SC, respectively; whereas, majority carriers move to the bulk of the SC. This generated electrons jumps into the conduction band creating holes in the valence band. The photogenerated holes are used to oxidize the species in Ist photoelectrode compartment and the electrons further moves towards the bulk of the semiconductor via metallic substrate travel into the another redox compartment where it is received by the oxidized species, and get reduced. These oxidized species acquires either reduced to lower oxidation state or to metal. These species can again be deoxidized by transferring an electron to the metal electrode in redox compartment, in dark while hole moves towards the surface of the semiconductor and accepted by the reduced species present in photoelectrode compartment, and get oxidized. In dark, these oxidized species accept electrons from redox compartment, resulted into the flow of electricity through external load.

The variation of voltage and current with time in charging and discharging modes of C|1 M (NaOH–Na_2S–S)|n-$CdIn_2S_4$||1 M $FeCl_3$|C SC-SEP storage cell is shown in Fig. 5. The storage cell formed with $FeCl_3$ electrolyte is charged continuously for 2 h with intensity of light 100 mW/cm^2. From Fig. 5, it is seen that, the rate of charging of the redox storage cell is not constant, but it increases exponentially up to 20 min and then up to 40 min it increases quite slowly, after that it is saturated as the charging time proceeds. Under short circuit conditions, or under certain loads, the electrons (in n-type SC) reach the counter electrode where they are used for the reduction of the oxidized species:

$$\text{red} + h^+ \rightarrow \text{oxi (at n-type semiconductor)}$$
$$\text{oxi} + e^- \rightarrow \text{red (at counter electrode).}$$

The associated electrode reactions during charging mode are given below, in photoelectrode compartment,

$$S^{2-} + 2h^+ \rightarrow S$$
$$S + S^{2-} \rightarrow {S_2}^{2-}$$

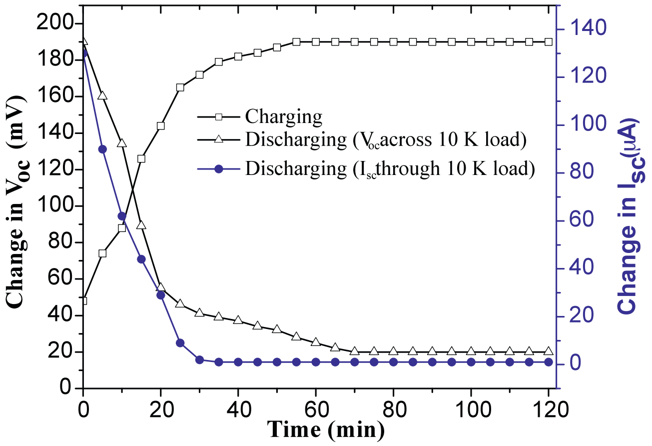

Fig. 6. Distinction between voltage and current versus time plots of the charging and discharging mode of C|1 M (NaOH–Na_2S–S)|$CdIn_2S_4$||1 M $K_4Fe(CN)_6$|C SC-SEP storage cell.

In the redox compartment,

$$Fe^{3+} + e^- \rightarrow Fe^{2+}$$

The discharging of storage cell is studied through a load resistance of 10 kΩ, measuring voltage and current in the external circuit. During discharging mode, both voltage and current decreases slowly with discharging time and attains constant value after 2 h of discharging time. In the discharging mode, the following reactions take place in the redox compartment,

$$Fe^{2+} \rightarrow Fe^{3+} + e^-$$

and in the photoelectrode compartment,

$${S_2}^{2-} + 2e^- \rightarrow 2S^-$$

Fig. 6 reveals the plot of voltage and current versus time of the charging and discharging behaviour of C|1 M (NaOH–Na_2S–S)|n-$CdIn_2S_4$||1 M $K_4Fe(CN)_6$|C SC-SEP storage cell. From Fig. 6, it is seen that, the rate of charging of the storage cell increases up to 55 min and then it saturates as the charging time proceeds. This charging and discharging is stable up to 2000 cycles.

The following reactions occurs in this combination during charging, in photoelectrode compartment,

$$S^{2-} + 2h^+ \rightarrow S$$
$$S + S^{2-} \rightarrow {S_2}^{2-}$$

and in redox compartment,

$$Fe(CN)_6{}^{3-} + e^- \rightarrow Fe(CN)_6{}^{4-}$$

During discharging, in redox compartment,

$$Fe(CN)_6{}^{4-} \rightarrow Fe(CN)_6{}^{3-} + e^-$$

and in photoelectrode compartment,

$${S_2}^{2-} + 2e^- \rightarrow 2S^-$$

The discharging rate of storage cell is relatively faster during first 20 min, and then it is quite slow. During charging, these reactions shift from left to right and vice versa. Thus the light energy is stored in form of the chemical energy of ${S_2}^{2-}$ ions. The amount of energy stored with time is studied by recording the voltage. The performance of semiconductor-septum storage cell with n-$CdIn_2S_4$ semiconductor separator in polysulphide with different electrolytes in redox compartment such as $FeCl_3$, $FeCl_2$, $K_3Fe(CN)_6$, $FeCl_2$/$FeCl_3$ are shown in Table 2. Finally it is perceived that the

Table 2
Changes in photovoltages during charging and photovoltages and photocurrents during discharging for different electrolytes.

Electrolyte in compartment-I	Electrolyte in compartment-II	Charging voltage for 2 h (mV)		After 2 h discharging			
		Initial	Final	Current (μA)		Voltage (mV)	
				Initial	Final	Initial	Final
C|1 M (NaOH–Na_2S–S)|n-$CdIn_2S_4$|SS	1 M $FeCl_3$|C	303	416	630	208	416	310
C|1 M (NaOH–Na_2S–S)|n-$CdIn_2S_4$|SS	1 M $K_4Fe(CN)_6$|C	48	190	130	02	190	20
C|1 M (NaOH–Na_2S–S)|n-$CdIn_2S_4$|SS	1 M $FeCl_3/FeCl_2$|C	402	501	165	112	501	388
C|1 M (NaOH–Na_2S–S)|n-$CdIn_2S_4$|SS	1 M $FeCl_2$|C	120	210	335	217	210	98

performance of storage cell is best for $FeCl_3$ electrolyte than others. This can be attributed to non-matching of the electrolyte with the semiconductor electrode as well as Fermi energy level of the electrolyte may be placed beyond the forbidden gap of the electrolyte.

4. Conclusions

The spray deposited photoactive n-$CdIn_2S_4$ thin film electrode on stainless steel substrates were successfully used in semiconductor-septum storage cell. The $FeCl_3$ redox electrolyte based storage cell shows better PEC conversion efficiency. The septum cell is stable up to 2000 charging and discharging cycles.

Acknowledgement

One of the authors (S.S. Shinde) is highly grateful to the DRDO for the Junior Research Fellowship through its project ERIP/ER/0503504/M/01/007.

References

[1] C. Amano, H. Sugiura, A. Yamomoto, M. Yamaguchi, Appl. Phys. Lett. 51 (1987) 1998.
[2] S.S. Shinde, P.S. Patil, R.S. Gaikwad, R.S. Mane, B.N. Pawar, K.Y. Rajpure, J. Alloys Compd. 503 (2010) 416.
[3] M. Okui, T. Nishizaki, M. Uno, K. Kurosaki, S. Yamanaka, K. Takeda, H. Anada, J. Alloys Compd. 330–332 (2002) 645.
[4] M. Armand, J.M. Tarascon, Nature 451 (2008) 652.
[5] J.M. Tarascon, M. Armand, Nature 414 (2001) 359.
[6] M.S. Whittingham, Chem. Rev. 104 (2004) 4271.
[7] K.R. Murali, V. Subramanian, N. Rangarajan, A.S. Lakshamanan, S.K. Rangarajan, Bull. Electrochem. 7 (1991) 230.
[8] M. Sharon, P. Veluchamy, C. Natarajan, D. kumar, Electrochim. Acta 136 (1999) 1107.
[9] H.T. Tien, Nature 227 (1970) 1232.
[10] H.T. Tien, J.W. Chen, Photochem. Photobiol. 49 (1989) 327.
[11] K. Jackowska, H.T. Tien, Solar Cells 23 (1988) 147.
[12] K. Xiao, H.T. Tien, Solar Cells 23 (1988) 233.
[13] K.Y. Rajpure, C.H. Bhosale, Mater. Chem. Phys. 64 (2000) 70.
[14] S.H. Pawar, M.P. Patil, V.N. Shinde, Bull. Electrochem. 9 (1993) 253.
[15] S.S. Dumure, C.D. Lokhande, Sol. Energy Mater. Sol. Cells 29 (1993) 183.
[16] S.H. Pawar, P.S. Patil, Bull. Electrochem. 6 (1990) 618.
[17] R.R. Sawant, C.H. Bhosale, Ind. J. Pure Appl. Phys. 44 (2006) 741.
[18] R.R. Sawant, S.S. Shinde, C.H. Bhosale, K.Y. Rajpure, Sol. Energy 84 (2010) 1208.
[19] R.R. Sawant, K.Y. Rajpure, C.H. Bhosale, Physica B 393 (2007) 249.
[20] L.P. Deshmukh, V.S. Sawant, P.P. Hankare, Sol. Cells 31 (1991) 557.